ACS APPLIED MATERIALS & INTERFACES

Research Article

www.acsami.org

Functionality of Proteins Bound to Plasma Polymer Surfaces

Bryan R. Coad,*[,†,‡] Tanja Scholz,[†] Krasimir Vasilev,[‡] John D. Hayball,[§,⊥,#] Robert D. Short,[‡] and Hans J. Griesser[†]

[†]Ian Wark Research Institute and [‡]Mawson Institute, University of South Australia, Mawson Lakes 5095 SA Australia

[§]Experimental Therapeutics Laboratory, Hanson Institute, Royal Adelaide Hospital, Adelaide SA 5000, Australia

[⊥]Sansom Institute, University of South Australia, Adelaide SA 5000, Australia

[#]School of Medicine, University of Adelaide, Adelaide SA 5000, Australia

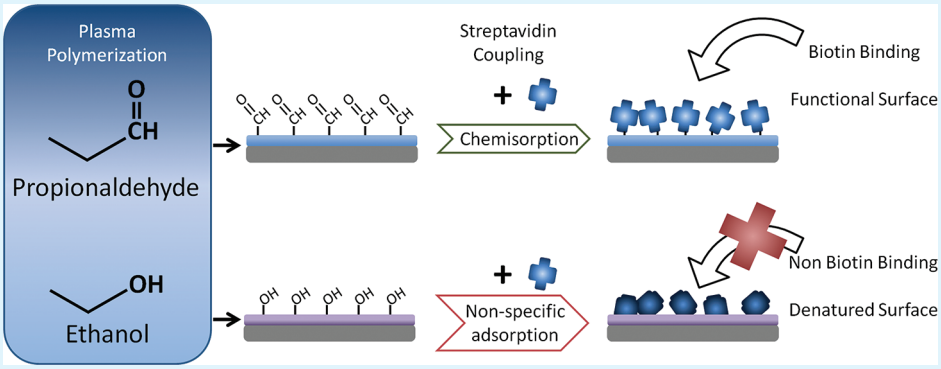

ABSTRACT: The deposition of a thin film layer by plasma polymerization enables the surface functionalization of a wide range of substrate materials for biointerfacial interactions. Plasma polymers can surface-bind proteins specifically via covalent linkages or nonspecifically through other irreversible adsorption mechanisms; key questions are whether covalent chemisorption has indeed occurred, and whether the protein retains functionality. Here the mode of surface binding of streptavidin and the biotin binding functionality of the bound streptavidin layer are studied on plasma polymer (pp) surfaces deposited using propionaldehyde and ethanol that were plasma polymerized at different powers (P) to investigate possible mechanisms for protein binding to a range of different surface chemistries. As expected, with pp surfaces composed principally of aldehyde groups, protein conjugation appears to be specific (chemisorption) allowing the immobilization of streptavidin (SAV) molecules retaining the ability to bind biotinylated probes. To contrast with this, we present the first study of protein adsorption to ethanol pp surfaces prepared at different P. This provides an investigation into retention of the hydroxyl functionality in the pp at low P and its effect on protein adsorption. Adsorption of human serum albumin (HSA) to ethanol pp was similar to that on propionaldehyde pp except at low P (5 W) where hydroxyl group retention and hydration presumably has a role in reducing protein adsorption. Although we observed SAV adsorption to ethanol pp surfaces at all P, interestingly, the protein lost its ability to bind biotinylated probes. Thus we suggest that irreversible, nonspecific adsorption of protein on ethanol pp surfaces results in apparent protein denaturation despite the hydrophilic nature of the ethanol pp surface. We conclude by making inferences between the pp structure as measured by X-ray photoelectron spectroscopy (XPS) and the related protein adsorption mechanisms.

KEYWORDS: *biomaterial interface engineering, plasma polymerization, bioconjugation, ethanol plasma polymer, propionaldehyde plasma polymer, aldehyde surface, biointerfaces, biomaterial surfaces, protein adsorption*

INTRODUCTION

The purpose of this work was to investigate protein adsorption to plasma polymers prepared from oxygen-containing organic vapors. By the use of surface characterization techniques and adsorption studies, we have found relationships between the amount of bound protein and its ability to retain functionality based on the chemical properties of the surface as modified by manipulation of the plasma polymerization power (P). The goal was to develop new insights into protein adsorption to plasma polymer surfaces to underpin applications such as the development of new diagnostic systems.[1,2]

Designed biomaterial coatings attempt to control the biological response at the materials/bio interface, and are created via the use of new fabrication strategies. Because protein adsorption occurs rapidly to surfaces the moment they are exposed to biological fluids a common first step in the development of new coatings is to evaluate protein adsorption.[3] Such coatings can be used to create new diagnostic devices.

Received: January 22, 2012
Accepted: April 10, 2012
Published: April 10, 2012

Diagnostic devices are an indispensible tool in health sciences research allowing for drug discovery and understanding fundamental biochemical pathways through the use of techniques such as enzyme linked immunosorbant assays (ELISA).[4] Coatings for in vitro diagnostic tools seek to improve specificity by utilizing directed immobilization strategies (chemisorption) while reducing nonspecific adsorption of proteins. Developing versatile manufacturing strategies for diagnostic devices relies upon providing a variety of chemical groups that favor chemisorption and understanding how the properties of the coating could influence irreversible, nonspecific adsorption as well as protein denaturation upon binding.

Plasma polymerization has shown utility and versatility as a bioconjugation platform.[1] This is due to its wide applicability to different substrates and customizability in the choice of providing many linking chemistries provided by different monomers. As a substrate independent coating methodology for example, plasma polymerization facilitates fabrication of functional coatings and scaffolds mediating biological response.[5] Previously we have shown the utility of aldehyde pp surfaces to form covalent linkages to lysine groups on proteins when fabricating bioconjugation platforms.[6,7] Reductive amination can be used in a two-step procedure that reduces the imine bond between aldehydes and amines to an amine bond; however, we found that imine bond formation is rapid and strong enough for our purposes, allowing for a simple conjugation protocol.[6] The advantage of this approach over others is that surface coupling is carried out in a single incubation step using only buffer and eliminates the possibility of surface contamination by reaction side products (e.g., urea derivatives in the case of carbodiimide) or reducing agents.[8] Because propionaldehyde can be easily plasma polymerized onto a wide variety of substrates, providing reactive aldehyde surface groups, this is an effective strategy for fabricating diagnostic tools based on chemisorption methods.[6,7,9]

Plasma polymers used for creating surfaces rich in hydroxyl groups have also been investigated. Such surfaces in the past have principally attracted attention due to the fact that cellular binding studies have shown them to be effective as cell-adherent surfaces.[10−14] The extent of cellular adhesion to hydroxylated surfaces, however, is not clear-cut as studies report different results, attributed to various experimental conditions. This is partly due to the indeterminate chemical functionality of oxygen in the plasma polymer; it could take the form of hydroxyl, ether, ester, carboxylic acid, arising from different monomers, plasma power (P), flow, reactor geometries, and atmospheric contaminants.[15] Additionally, the mechanism of cellular binding to surfaces is quite complex with the role of adsorbed proteins being an important factor mediating attachment.[11,16] Compared to aldehyde groups, which provide a specific linking chemistry to nucleophiles on proteins, hydroxyl groups are more chemically inert and bioconjugation is more likely to occur through physisorption.

It seems that more fundamental studies investigating protein adsorption to plasma polymers are needed. These studies are important because the protein adsorption mechanisms to hydroxyl surfaces again are not clear. As others have observed, the nature of the protein itself in addition to the chemistry of the surface will affect the bound amount,[17] suggesting that the structure and folding of the protein are important determinants. Disruption of higher-order protein structure could also have important consequences for protein activity. Notably, Bullett et al. found a comparatively high antibody response to IgG adsorbed to mixed acrylic acid/octadiene pp surfaces, which was inversely correlated to the analytically determined bound amount.[18] These two studies suggest that further investigation into the interplay between pp structure and protein activity is warranted.

One way to investigate variation of pp structure is to study the deposition of a given monomer under a constant set of plasma conditions except varying P. For other alcohol containing monomers such as allyl alcohol, low P plasmas were shown to increase the functional group retention (hydroxyl) on the surface.[19] In the case of protein adsorption, one might speculate that the type of surface containing many hydrophilic alcohol moieties may play a role in surface hydration, which could act as a barrier to preventing surface adsorption of protein as is the case with PEG-type polymers.[20] Thus, a P dependence study using ethanol suggests an intriguing hypothesis: Can ethanol pp surfaces be prepared through P variation to reduce the amount of protein adsorption to the surface?

We have only found one previous description of plasma polymerization of ethanol[21] and no previous report of protein adsorption studies. This is interesting because ethanol seems to be notably absent from the list of other simple, saturated, high-vapor pressure alcohols already studied (see ref 1, giving a summary of plasma polymerization of other alcohols including methanol, 1-propanol, isopropanol, isobutanol, and others). Conversely, allyl alcohol plasma polymers have been well-studied;[17,19,22−24] however, such a protein adsorption study as described above has not been attempted.

In this paper, we characterize protein adsorption and activity to propionaldehyde and ethanol pp surfaces. The presence of either aldehyde or hydroxyl groups provide a comparative basis for two possible mechanisms for the binding of these proteins to the two pp surfaces. We would expect binding to aldehyde surfaces should occur specifically (chemisorption) through formation of covalent imine linkages as demonstrated previously[6,9] whereas adsorption to ethanol surfaces probably occurs nonspecifically, unless that surface also contained aldehyde groups as a result of chemical reactions in the plasma deposition process. We investigate this hypothesis using a model protein, human serum albumin (HSA) and a biotin-binding protein, streptavidin (SAV). Results from adsorption studies and XPS surface characterization provide insights into possible adsorption mechanisms relating to protein functionality correlated with varying pp structure at decreasing P.

EXPERIMENTAL SECTION

Materials. All water used was purified (>18 MΩ cm) by use of a P.Nix UP 900 purification system (Human Corp. S. Korea). Propionaldehyde (reagent grade, 97%), PBS tablets, poly(allylamine hydrochloride) $M_w \approx 15\,000$, human serum albumin (>99%), and streptavidin (91.4% protein) were obtained from Sigma Aldrich Australia. Ethanol (absolute 99.5% v/v) was supplied by Ajax Finechem, NSW Australia. Thermanox coverslips (22 × 60 mm) were supplied by ProSciTech, QLD Australia. FlexiPERM micro 12 wells were supplied by Sarstedt, SA Australia. Sodium dodecyl sulfate (90%) was supplied by Chem-Supply, SA Australia. Gold nanoparticles, biotin labeled (0.05% Au w/v, 10 nm) were supplied by Nanocs Inc., NY, USA.

Plasma Polymerization. The deposition of a thin polymeric coating by gas plasma polymerization was performed as previously reported[25] using a custom-built plasma reactor[26] operated with a 13.56 MHz power generator and matching network. Plasma power was set

using the digital gauge reading and may not account for the actual delivered power through losses present in the construction of the reactor and cabling. Thermanox coverslips were first treated with a precoat of ethanol plasma polymer (0.20 Torr initial monomer pressure, plasma generated at 40 W for 4 min) to provide an initial surface coating approximately 15−20 nm thick as determined on identical plasma coatings on silicon wafer samples by ellipsometry. Then secondary plasma coatings of propionaldehyde or ethanol were coated on top at variable *P* from 40 to 5 W with an initial monomer pressure set to 0.20 Torr. The rate of plasma polymer deposition slows at low *P* (Figure 1). To ensure that we obtained layer thicknesses greater than the XPS sampling depth, we first determined the minimum deposition time required for either plasma polymer to coat an overlayer of about 15 nm. Ethanol plasmas were deposited for times ranging from 1 to 9 min and propionaldehyde plasmas were deposited for 0.5−4.25 min for the ranges of *P* studied (40 W down to 5 W respectively).

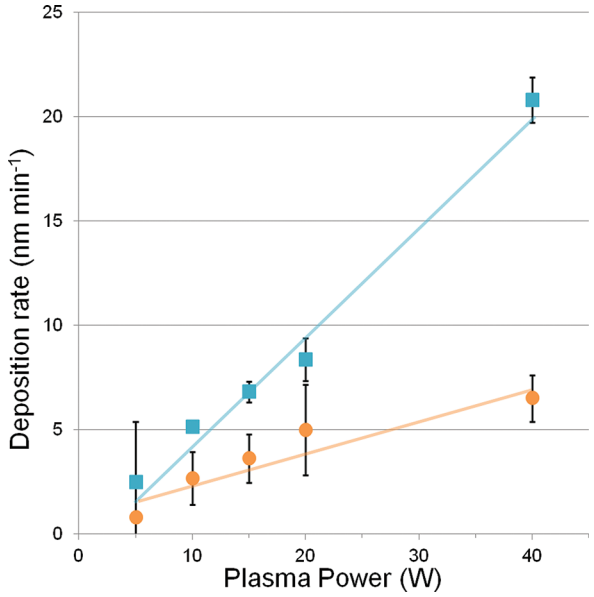

Figure 1. Deposition rates for propionaldehyde (blue squares) and ethanol (orange circles) plasma polymers at different applied pressures. The initial monomer pressure was 0.2 Torr. Error bars represent the standard deviation (n = 3). Lines represent linear regression of the data.

Surface Adsorption and Washing. Proteins were dissolved in PBS (0.1 mg mL^{-1}) and incubated with pp surfaces for 1 h at room temperature. After incubation, protein solutions were aspirated and washed once with PBS solution. SDS solution (0.01 M) was added and left for 1 h. After aspirating, surfaces were washed 6 times with PBS and finally rinsed with generous amounts of water. For binding assays on SAV surfaces, biotinylated gold nanoparticles were diluted 20 times and allowed to bind for 4 h at room temperature. Washing was performed by the same procedure described above.

Thickness Measurements. Plasma polymer thickness on silicon wafers was determined though the use of an imaging ellipsometer (Beaglehole Instruments, New Zealand). Measurement of reflected light (600 nm) was obtained at nine angles between 40 and 80 degrees. Thickness of plasma polymers was calculated by fitting the measured data to a four-layer model (Si/SiO_2/pp/air). The optical properties of the silicon substrate ($\varepsilon' = 15.60177$ and $\varepsilon'' = 0.2133$) and the native oxide layer ($\varepsilon' = 2.1357$ and $\varepsilon'' = 0$) were taken from the software (TFCompanion, Semiconsoft). A refractive index of 1.55 was assumed for all pp layers. This refractive index is in the range of the refractive indices reported in the literature for similar pps[27] and produced the best fit to the experimental data.

X-ray Photoelectron Spectroscopy. Coated samples were analyzed for their surface chemical compositions using a Kratos Axis Ultra DLD spectrometer equipped with a monochromatic Al Kα source. Charging of the samples during irradiation was reduced by an internal flood gun. Each sample was analyzed at an emission angle normal to the sample surface. Survey spectra were acquired at 120 eV pass energy of and high-resolution C 1s spectra were recorded at 20 eV pass energy. Data were processed with CasaXPS (ver.2.3.14 Casa Software Ltd.) with residuals for curve fits minimized with multiple iterations using simplex algorithms. Errors presented from survey and high-resolution spectra are the standard deviation values calculated within the software. These areas represent the uncertainty in the choice of fitting parameters to accurately model the peak areas and are generated using a Monte Carlo simulation method. Spectra were corrected for charge compensation effects by offsetting the binding energy relative to the C−C component of the C 1s spectrum which was set to 285.0 eV.

RESULTS AND DISCUSSION

Propionaldehyde and ethanol are both saturated organic compounds providing good model compounds of aldehyde and primary hydroxyl functionality. They are also good candidates for plasma polymerization since both are stable, relatively low molecular weight liquids at room temperature with relatively high vapor pressures. Propionaldehyde pp has been studied before and it has shown utility in the fabrication of bioconjugation platforms.[1,6,25] Investigation of ethanol pps are few[21] with no reports describing interfacial exposure to protein solutions. In the following sections, we describe a comparative analysis of these two pp surfaces when prepared at different power. Then we show surface characterization data after exposing to protein solutions. The functionality of SAV-coupled surfaces was then assessed by attempting to bind biotinylated probe nanoparticles. Finally, we present the results of binding amine-containing, nonproteinaceous polymers to pp surfaces and discuss the possible mechanisms affecting protein denaturation on ethanol pp surfaces.

Characteristics of Ethanol and Propionaldehyde pps. The deposition rate on silicon wafers was measured for plasma polymers as a function of *P*. Figure 1 shows the rate of thickness increase (nm min^{-1}) at different applied *P*. Comparatively, ethanol pp was found to have a slower deposition rate than propionaldehyde, particularly noticeable at high *P* where deposition occurs three times faster for propionaldehyde. In general, relatively slow deposition rates are not unexpected for pps from saturated compounds particularly when compared to their unsaturated homologues.[28] Regardless, the thickness of either pp could be easily controlled because the deposition rate was linear with *P*.

Figure 2 is a comparison of C 1s high-resolution XPS spectra for ethanol and propionaldehyde pps at the highest and lowest *P* studied. Spectra were fitted with three components giving a profile of the chemical environment of the surface as being mainly hydrocarbon (C1 component, 285.0 eV), ether or hydroxyl (C2 component, 286.0 eV), and carbonyl (C3 component, 287.9 eV). Comparison of the high power spectra (40 W) showed similar traces for both propionaldehyde and ethanol pp. For the spectra from surfaces produced at low *P* (5 W) there was a notable difference in proportion of the two oxygen−carbon components between the two plasma polymers. The fate of oxygen in these plasma polymers is discussed in detail below.

Notably absent were higher energy carbon−oxygen environments (carboxylic acid and ester) indicating that higher-order

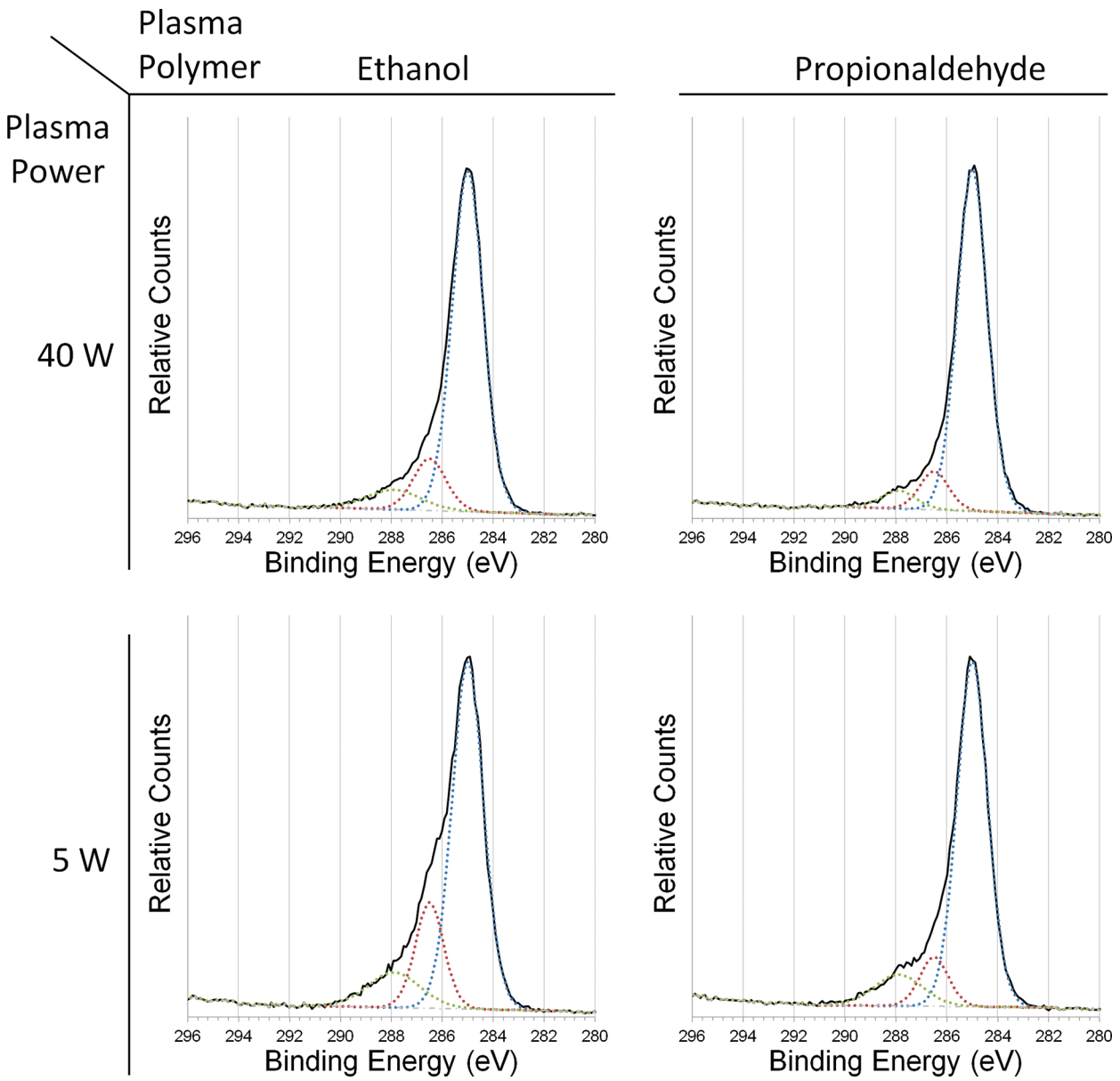

Figure 2. XPS high-resolution C 1s spectra. Plasma polymers from the two compounds studied (ethanol and propionaldehyde) are compared at the highest (40 W) and lowest (5 W) powers studied. Dashed lines are the model components used to fit the traces representing C1 (C−C, blue), C2 (C−O−C or C−O, red), and C3 (C═O, green).

oxidation states were not produced in the plasma. Previous studies have shown fairly significant carboxylic acid content in both methanol[11] and ethanol pp,[21] and to a lesser extent in 1-propanol pp.[29] Differences between these reports and the present one probably result because of the different operational conditions used. The absence of carboxylic acid in this study eliminates it as a potential binding mechanism.

When exposed to aqueous solutions, both pp surfaces were hydrophilic. The receding contact angle (RCA) for water on propionaldehyde pp surfaces was generally slightly higher than on ethanol pp surfaces. For sake of comparison on 20 W samples, the RCA for propionaldehyde pp was approximately 58° compared with approximately 30° for ethanol pp.

Fate of Oxygen. Figure 3 shows oxygen to carbon peak areas from XPS wide scan analysis for ethanol plasma polymer (A) and propionaldehyde plasma polymer (B) as a function of *P*. The uppermost bars trace the total oxygen content from the survey spectrum normalized to carbon content. The fate of the oxygen in the plasma polymers can be determined by examining the peak areas fitted from high resolution XPS C 1s spectra (lower two bars). These correspond to normalized peak areas for the C2 component (C−O or C−O−C, red line) and the C3 component (C═O, green line).

Compared to the composition of the intact parent compound, data from the survey spectra show that ethanol and propionaldehyde pps were comparatively deficient in oxygen. At 40 W, elimination of oxygen occurred to the greatest extent (topmost orange bars in Figure 3) for ethanol, where O/C was 0.16 (theoretical maximum 0.5), and propionaldehyde, where O/C was 0.13 (theoretical maximum 0.33). Reducing the power resulted in more oxygen incorporation with values at 5 W of 0.28 for ethanol (56% of the maximum theoretical value) and 0.19 for propionaldehyde (58% of the maximum theoretical value). The mechanism for oxygen loss may be

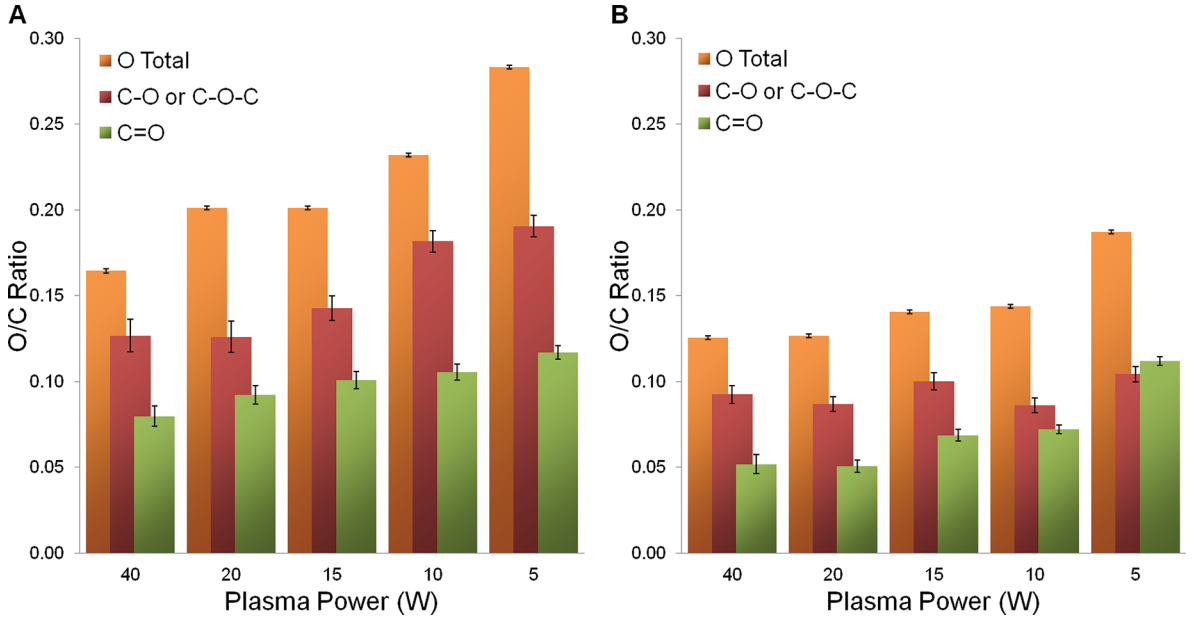

Figure 3. Oxygen fate in (A) ethanol plasma polymer and (B) propionaldehyde plasma polymer at different applied powers. Total oxygen peak area (orange) from XPS survey spectrum, normalized against total carbon peak area. XPS C 1s component peak areas for C2 (C−O or C−O−C in red) and C3 (C═O in green) normalized against the total C 1s peak area.

related to elimination of carbon-oxides in the gas phase or through elimination of water.[21] Water elimination seems to be an energetically favorable elimination pathway at least for other alcohols such as 2-propanol because the resulting plasma polymer is able to stabilize the loss of a secondary hydroxyl group, leading to comparatively higher oxygen loss.[22]

As for the oxygen remaining on the surface, quantification of the peak areas fitted to the high-resolution spectra allow for some discussion on the oxygen fate and resulting chemical composition of the surfaces. As mentioned above, we only observed three distinct carbon−oxygen peaks representing hydrocarbon (C1) ether or alcohol (C2) and carbonyl (C3) for both plasma polymers at all *P*. For ethanol pp at lower values of *P*, the increasing oxygen content in the plasma polymer contributes nearly equally to increases in C2 and C3 component areas (Figure 3A, red and green bars, respectively) resulting in a value for C2/C3 which is nearly constant. This was quite different when compared to propionaldehyde pp (Figure 3B). As *P* was decreased, the increasing oxygen content contributed more to the C3 peak area, giving C2/C3, which decreased and became less than 1 at 5 W. The marked upturn in the C3 component at this point indicated that at this *P*, a greater (although not statistically significant) proportion of the aldehyde functionality was retained. On the whole, the data suggests a trend toward aldehyde functionality becoming the dominant C−O chemical environment in this pp at low *P*.

Although it is not possible to resolve ether and alcohol peaks, there may be reason to arrive at a similar conclusion for ethanol pp; that is, lower *P* surfaces should contain a greater proportion of hydroxyl groups compared to the higher *P* surfaces. In ethanol pp, high O/C ratios (approaching 0.3) were suggested to be in better theoretical agreement with O forming only one bond to carbon (i.e., hydroxyls) rather than a two-bond arrangement (ethers or epoxides) where the O/C ratio would be expected to be much lower.[21] Also, in allyl alcohol pps, labeling studies showed that at lower *P*, a greater quantity of hydroxyl is present compared to pps derived under high *P* conditions.[22] Therefore, it seems a reasonable hypothesis to suggest that our low *P* ethanol pp surfaces contain significant hydroxyl character.

Characteristics of Model Proteins Used in Adsorption Experiments. In this study, we have characterized protein adsorption to surfaces by XPS and speculated on the role of the primary and secondary protein sequences. We chose human serum albumin (HSA) and streptavidin (SAV) as representative proteins used in this study. Table 1 provides protein data relevant to this discussion. SAV used in this study was bacterially expressed from *Streptomyces avidinii* and purified using biotin affinity chromatography. It is a functional model protein representing a class of biotin-binding molecules useful in bioconjugation and ELISA applications.[30−32] Human serum albumin (HSA) was chosen for its use as a model glycoprotein of average molecular weight and its use in this regard has been well-studied. HSA and SAV both contain around 18% N (observable by XPS) and have similar values of N/C (Table 1). A major difference between these two proteins is the number of lysine residues present per molecule. For HSA, we would

Table 1. Physical Properties of Proteins Used in Adsorption Experiments

	HSA[a]	SAV[b]
subunit MW		13 300
mol wt (Da)	66 500	53 000
max observable N % by XPS[c]	17.8	18.5
N/C ratio	0.312	0.325
no. of lysine residues per molecule	59	16
no. of accessible lysine residues per molecule	47−51[d]	16[e]
glycans associated with protein	present	absent

[a]Sequence data from RSCB Protein Data Bank 1E7H[34] [b]Sequence data from RSCB Protein Data Bank for "apo-core streptavidin" 1SWB[35] [c]Nitrogen percentages calculated from empirical protein formula omitting hydrogen. [d]Based on experimental conjugation studies.[33] [e]Estimated from 3D crystal structure.

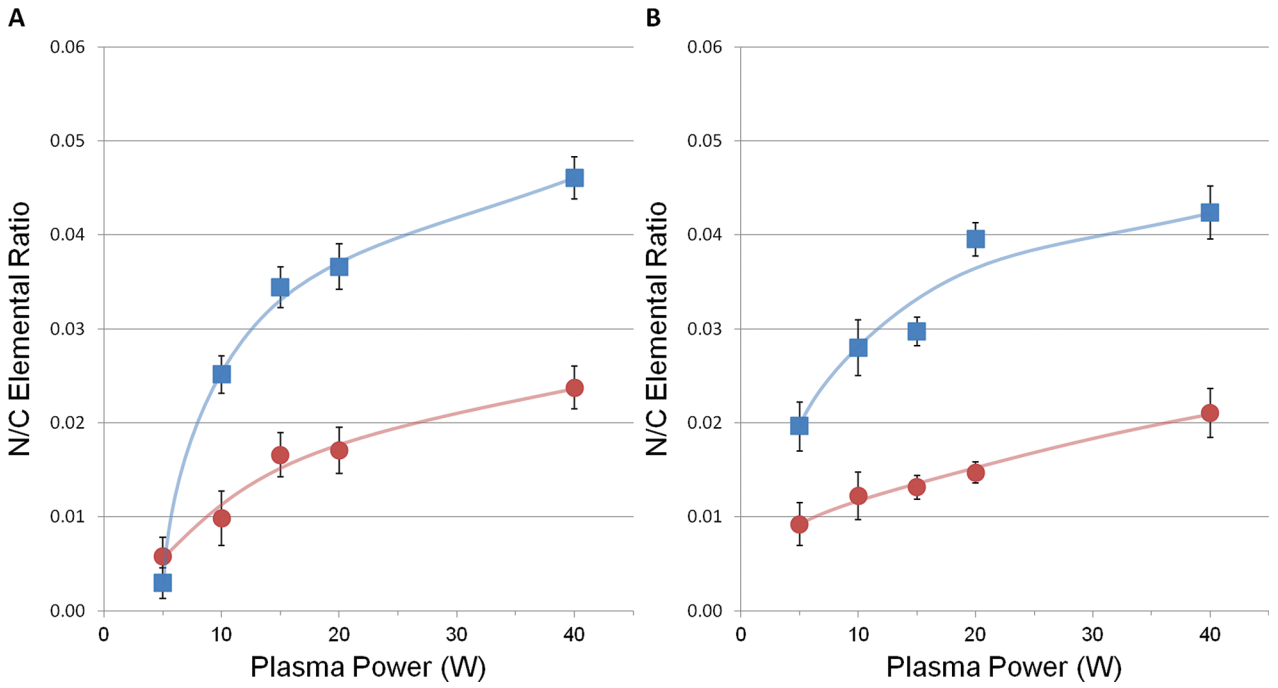

Figure 4. Protein adsorption (blue squares, HSA; red circles, SAV) as measured by the XPS N/C elemental ratio to plasma polymer surfaces. (A) Ethanol pp and (B) propionaldehyde pp. Lines are presented to guide the eye.

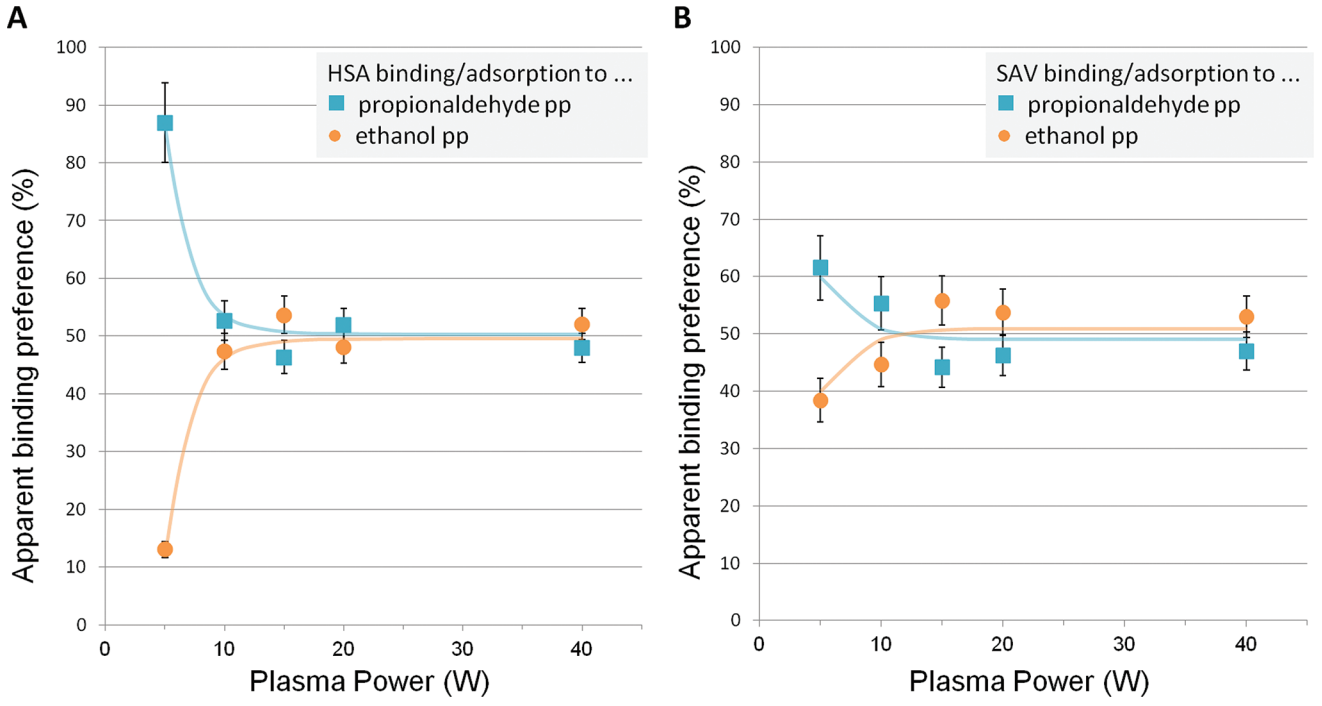

Figure 5. Apparent preference for (A) HSA adsorption and (B) SAV adsorption to (blue squares) propionaldehyde and (orange circles) ethanol pp surfaces. Apparent adsorption preference is expressed as a percentage of the total N/C value for the protein at a given plasma power from the data in Figure 4. Lines are presented to guide the eye.

expect that each molecule would present approximately 47−51 lysine residues as potential anchors for surface immobilization.[33] SAV contains about three times less lysines per molecules. This is an important difference that potentially affects specific modes of surface conjugation for either protein as discussed below.

Protein Adsorption Studies. Solutions of protein were exposed to either plasma polymer surface for a given incubation period, extracted then washed. Figure 4 gives the XPS N/C elemental ratio for these surfaces. Results indicate that adsorbed proteins (HSA or SAV) were detected on both the ethanol pp (A) and the propionaldehyde pp (B). We would expect that only protein that was chemically linked (chemisorbed) or adsorbed irreversibly (nonspecifically) remained at the surface since soaking with a surfactant and extensive rinsing was used in the washing procedure. A trend to decreasing protein

adsorption with decreasing P was observed for both surfaces. For ethanol pp, protein adsorption appeared to decrease rapidly for $P < 20$ W with detected protein approaching zero at $P = 5$ W (Figure 4A). Protein adsorption to propionaldehyde pp surfaces was also found to decrease with decreasing P; however, the rate of decrease was noticeably less, with a greater amount of protein detected on 5 W pp surfaces compared to the ethanol case (Figure 4B). This difference in detected protein suggests differing protein binding mechanisms related to the low-power structure of either of the plasma polymers. As we have created surfaces with low and high amounts of alcohol and aldehyde functionalities, we can relate the plasma polymer structure to possible binding mechanisms in a discussion comparing the apparent protein adsorption preference to either surface.

Apparent Protein Adsorption Preference on Ethanol and Propionaldehyde pp Surfaces. The apparent protein adsorption preference (Figure 5) is a representation of the data from Figure 4 showing the pp surface to which binding would be expected (high percentage values) or to which a lack of binding would be expected (low values) as a function of P. This was calculated as follows: the total N/C value for both proteins on either surface was calculated (i.e., sum of N/C at each value of P shown in Figure 4A and B) and then the N/C value for each protein was expressed as a percentage of this sum at each value of P. Here we see that HSA (Figure 5A) would apparently bind equally well (equal amounts) to either pp surface within experimental error at all P from 40 W down to 10 W. At 5 W, there was a strong apparent preference for binding to propionaldehyde surfaces. Another interpretation of this is that there was a strong apparent prevention of adsorption to ethanol pp surfaces. There is a physical basis supporting these observations in the arguments regarding retention of hydroxyl and aldehyde functional groups deduced above. First, at 5 W, where we suggested the best evidence for functional group retention, alcohol groups presumably played a role in reducing protein adsorption to the surface, giving a low preferential binding to ethanol surfaces. Second, increased aldehyde functionality facilitated chemisorption to propionaldehyde surfaces giving a high observed preferential binding.

The same can be said for SAV adsorption (Figure 5B) excepting that the magnitude of this effect was diminished and that the onset of preferential binding seems to become more apparent at slightly higher P (10 W). This reduction in magnitude in binding preference is simply a reflection of the lower amount of nitrogen detected for adsorbed SAV compared to HSA. However, the apparent binding trend is similar for both proteins.

The reason for the smaller quantified amount of SAV compared to HSA raises interesting questions about possible binding mechanisms. For example, if the same number of SAV and HSA molecules had bound to propionaldehyde surfaces, we know from Table 1 that the detected N/C ratio would be about the same. One possible explanation for the lower N/C values for SAV could arise from the fact that SAV has fewer lysine residues available to facilitate conjugation to aldehyde groups. Therefore, there could be a kinetic limitation in covalent bond formation. As we have described, 5 W propionaldehyde pp surfaces represent surfaces with significant aldehyde character, therefore it makes sense that these surfaces would provide better opportunity for covalent attachment of proteins with a greater number of lysine residues (HSA, Figure 5A) compared to SAV (Figure 5B) . It is possible that the protein secondary structure provides another mechanism of adsorption to the surface (e.g., nonspecifically through physisorption). Next, we present evidence showing this to be an additional, important factor to consider in protein binding and functionality to these pp surfaces

Biotin–Gold Nanoparticle Binding to Immobilized SAV. Since irreversible, nonspecific protein adsorption to surfaces is a potential binding mechanism which could result in possible protein denaturation, we have used a functional protein (SAV) to gauge its ability to bind biotinylated probes after immobilization. As our ligand probe, we chose biotinylated gold nanoparticles as these entities provide a convenient way to add a unique "tracer" element onto the surface for the purpose of XPS quantification. Figure 6 graphs

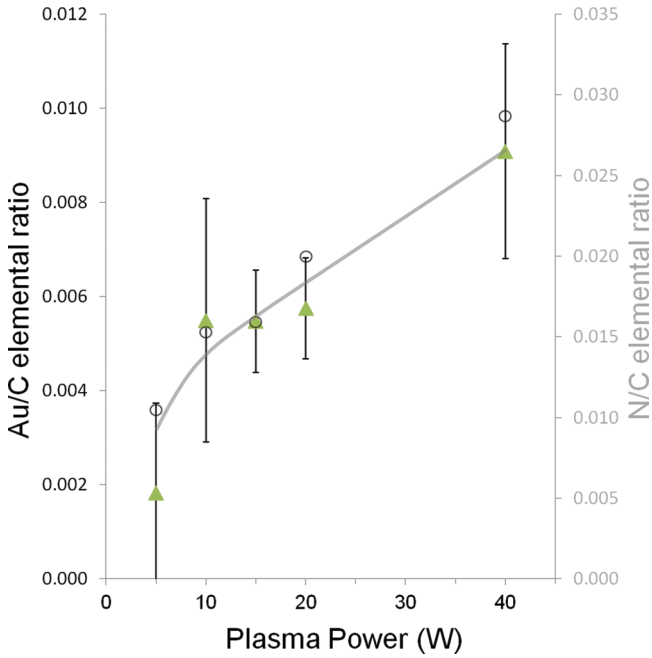

Figure 6. Biotin–gold nanoparticle binding (green triangles) to SAV on surfaces prepared from propionaldehyde pp analyzed by Au/C elemental ratio (left-hand vertical axis). For comparison, the data are overlaid with the N/C elemental ratio from immobilized SAV plotted as faded data points (circle) with a line to guide the eye, plotted in relation to the faded N/C elemental ratio scale on the right-hand vertical axis.

the Au/C elemental ratio for propionaldehyde pp surfaces bound with SAV and then exposed to solutions of biotinylated gold nanoparticles at different P. Gold present on the surface is indicative that the biotinylated nanoparticle probe has bound to immobilized, functional SAV. For comparison sake, the N/C data from Figure 4B (SAV adsorption to the same surface) is also plotted here but on a different scale (right-hand vertical axis) as faded points with a line to guide the eye to the trend. The decreasing Au/C ratio shows a decreasing amount of gold bound to the surface with lower P and this reflects the trend seen with bound SAV. The retained functionality of the protein suggests that aldehyde groups present on the surface provided a specific adsorption mechanism (i.e., chemisorption) resulting in an effective platform for protein linking.

We applied the same diagnostic assay to ethanol pp surfaces with adsorbed SAV. Interestingly, we were not able to detect any gold signal for binding to SAV on coatings deposited under

all *P* studied. One possible interpretation is that the adsorbed SAV is incapable of binding biotin due to denaturation by conformational changes. However, absence of binding of biotinylated gold NPs could alternatively be caused by delamination, partially or entirely, of the ethanol plasma polymer layer, which would also remove the adsorbed SAV. To exclude this possibility, we have assessed samples after extended solvent exposure (24 h) and washing conditions used in the present work. XPS spectra were unchanged, with no substrate signals. In addition, the film thickness was measured by ellipsometry and we found that for coatings deposited under a similar range of plasma powers down to 10 W, identical film thicknesses were measured both before and after solution exposure. Thus, clearly, the ethanol pp coatings are stable under the conditions of this study. XPS analysis also confirmed that SAV remained bound since the measured N/C values after solution exposure and after exposure of samples to the nanoparticle binding assay were essentially the same as those shown in Figure 4A; although no Au signal was detected, N was (data not shown). Because we thus know that SAV was present on the ethanol pp surfaces and was not washed off during the biotinylated gold nanoparticle assay, we conclude that the adsorbed protein lost its functional ability to bind biotinylated probes.

Until now, we have not speculated on possible nonspecific adsorption mechanisms for proteins to ethanol pp surfaces. Although higher energy carbon−oxygen binding environments were evident, including an approximately 10% abundance of C═O present at all *P* studied, in general, ethanol pp contained much higher levels of ether or alcohol (15 to 20%) with the majority being hydrocarbon (70 to 75%) . The undefined and largely hydrocarbon-rich structure of ethanol pp films may allow surface adsorption to occur through van der Waals forces. To investigate the role that a protein's physical properties and secondary structure could play in nonspecific adsorption, we performed adsorption studies using a nonpolypeptide probe, poly(allylamine) (pAla), as a model of a simple, primary amine-containing linear polymer chain that has the additional benefit of high water solubility and thus is unlikely to bind to hydrophilic surfaces in the absence of chemical bond formation. The observation of C═O groups in the XPS C 1s spectrum of ethanol pps raises the possibility that the ethanol pp surface might contain, in addition to hydroxyls, some aldehyde groups due to reactions within the plasma. If so, the ethanol pp should be able to bind the highly water-soluble pAla, whereas in the absence of aldehyde groups we would expect no binding of pAla as its nonspecific adsorption to hydrophilic uncharged surfaces should be minimal.

Poly(allylamine) Binding. Figure 7 gives the N/C elemental ratio from XPS survey spectra for poly(allylamine) on propionaldehyde pp surfaces at different *P*. The binding trend for this synthetic polymer was similar to that seen with proteins. One would expect that aldehyde groups facilitated conjugation to primary amines present on the pAla, resulting in covalent attachment.

Binding of pAla was also attempted onto ethanol pp surfaces; however, no nitrogen signal was detected, indicating that adsorption did not occur (data not shown). This finding indicates that the density of aldehyde surface groups on the ethanol pp must be negligible. Therefore the C═O component observed in the XPS C 1s spectrum is due to ketone structures which, unlike aldehyde groups, are not capable of covalent interfacial bond formation under our binding conditions.

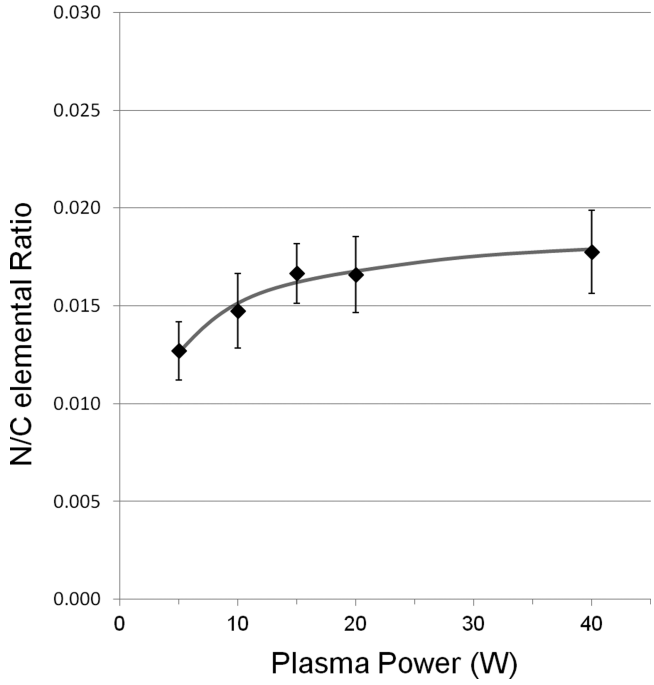

Figure 7. Poly(allylamine) binding to propionaldehyde pp surfaces as measured by the XPS N/C elemental ratio. A line has been presented to guide the eye.

The fact that biopolymers such as HSA and SAV can adsorb to ethanol pp surfaces while pAla does not suggest that the adsorption of proteins is related to the primary and secondary structure of the polypeptide chain. Therefore, possible mechanisms of adsorption could include hydrophobic, dipole, or dispersion forces between amino acid residues or structural domains and the surface. Because biotin binding to streptavidin is made possible through hydrophobic pockets present at the binding sites, it would be interesting to investigate possible mechanisms of structural disruption specifically in these areas in relation to adsorption to pp surfaces.

CONCLUSIONS

We have studied ethanol and propionaldehyde plasma polymer films at different power levels. Decreasing plasma power resulted in a greater amount of oxygen incorporated into the plasma polymer. At low power levels (5 W) XPS spectra showed evidence that the respective (alcohol or aldehyde) functional groups were retained as the dominant oxygen-containing species bound to carbon. At higher powers up to 40 W, it was difficult to make inferences of either pp structure other than the fact that the different proportions of oxygen and oxygen-bound-to-carbon in ethanol and propionaldehyde suggested quite different pp composition.

We hypothesized that ethanol pp should contain alcohol-like functionality that might reduce nonspecific adsorption of proteins while propionaldehyde would allow protein binding through the formation of imine bonds. At the power where we saw clear structural retention (5 W), data showed that comparatively, propionaldehyde pp surfaces showed a much greater apparent binding preference for proteins and a nitrogen containing synthetic polymer while ethanol pp surfaces showed a lack of preference for adsorbing these species. Although low and approaching zero, a small amount of protein adsorption occurred on ethanol pps as the power was decreased. At higher

power, protein adsorption was seen to plateau to a level nearly equal to that of propionaldehyde pp. Here, adsorption to either pp was nonpreferential although the mechanism was different.

SAV was attached to aldehyde groups on propionaldehyde pp surfaces resulting in retention of the protein's biotin-binding ability. However, protein (SAV) exposure to ethanol plasma polymer surfaces resulted in probable protein denaturation resulting in an inability to bind biotinylated molecules. This highlights the differences in the functionality of the aldehyde-based and hydroxyl-based surfaces. Because the amine-containing synthetic polymer polyallylamine (i.e., a nonprotein) was able to bind to aldehyde surfaces but not to ethanol surfaces we conclude that specific covalent coupling is facilitated through imine bond formation on the former whereas the ethanol plasma polymer surface does not contain aldehyde groups and cannot bind amines covalently. Adsorption to ethanol plasma polymer surfaces must be related to the properties of the polypeptide's structure. Because polypeptides have the potential to physisorb to surfaces by way of van der Waals forces, and the fact that strong adsorption can lead to denaturation of the protein, we offer this as an explanation for the mechanism of binding and the lack of protein functionality observed on ethanol pp surfaces. The different mechanisms of adsorption (specific covalent binding in one case and irreversible, nonspecific adsorption with apparent denaturation in the other) could have interesting consequences when preparing bioconjugation platforms from these plasma polymers.

AUTHOR INFORMATION

Corresponding Author

*E-mail: Bryan.Coad@unisa.edu.au.

Notes

The authors declare no competing financial interest.

ACKNOWLEDGMENTS

We acknowledge funding from the National Health and Medical Research Council, Australia, under Grant ID 631931.

REFERENCES

(1) Siow, K. S.; Britcher, L.; Kumar, S.; Griesser, H. J. *Plasma Process. Polym.* **2006**, *3* (6−7), 392−418.
(2) Kim, M. S.; Khang, G.; Lee, H. B. *Prog. Polym. Sci.* **2008**, *33* (1), 138−164.
(3) Ratner, B. D.; Bryant, S. J. *Annu. Rev. Biomed. Eng.* **2004**, *6*, 41−75.
(4) Crowther, J. R., *ELISA: Theory and Practice*; Humana Press: Totowa, NJ, 1995; Vol. *42*, p 223.
(5) Coad, B. R.; Lu, Y.; Meagher, L. *Acta Biomater.* **2012**, *8* (2), 608−618.
(6) Diener, K. R.; Christo, S. N.; Griesser, S. S.; Sarvestani, G. T.; Vasilev, K.; Griesser, H. J.; Hayball, J. D. *Acta Biomater.* **2012**, *8* (1), 99−107.
(7) Christo, S. N.; Sarvestani, G. T.; Griesser, S. S.; Coad, B. R.; Griesser, H. J.; Vasilev, K.; Brown, M. P.; Diener, K. R.; Hayball, J. D. *Aust. J. Chem.* **2012**, *65*, 45−49.
(8) Hermanson, G. T., *Bioconjugate Techniques*, 2nd ed.; Academic Press: London, 2008; p 1202.
(9) Coad, B. R.; Vasilev, K.; Diener, K. R.; Hayball, J. D.; Short, R. D.; Griesser, H. J. *Langmuir* **2012**, *28* (5), 2710−2717.
(10) Curtis, A. S. G.; Forrester, J. V.; Clark, P. *J. Cell Sci.* **1986**, *86*, 9−24.
(11) Ertel, S. I.; Ratner, B. D.; Horbett, T. A. *J. Biomed. Mater. Res.* **1990**, *24* (12), 1637−1659.
(12) Ertel, S. I.; Chilkoti, A.; Horbett, T. A.; Ratner, B. D. *J. Biomater. Sci.-Polym. Ed.* **1991**, *3* (2), 163−183.
(13) Guerin, D. C.; Hinshelwood, D. D.; Monolache, S.; Denes, F. S.; Shamamian, V. A. *Langmuir* **2002**, *18* (10), 4118−4123.
(14) Mitchell, S. A.; Davidson, M. R.; Emmison, N.; Bradley, R. H. *Surf. Sci.* **2004**, *561* (1), 110−120.
(15) Daw, R.; Candan, S.; Beck, A. J.; Devlin, A. J.; Brook, I. M.; MacNeil, S.; Dawson, R. A.; Short, R. D. *Biomaterials* **1998**, *19* (19), 1717−1725.
(16) Malik, A. F.; Hoque, R.; Ouyang, X.; Ghani, A.; Hong, E.; Khan, K.; Moore, L. B.; Ng, G.; Munro, F.; Flavell, R. A.; Shi, Y.; Kyriakides, T. R.; Mehal, W. Z. *Proc. Natl. Acad. Sci. U.S.A.* **2011**, *108* (50), 20095−20100.
(17) Whittle, J. D.; Bullett, N. A.; Short, R. D.; Douglas, C. W. I.; Hollander, A. P.; Davies, J. *J. Mater. Chem.* **2002**, *12* (9), 2726−2732.
(18) Bullett, N. A.; Whittle, J. D.; Short, R. D.; Douglas, C. W. I. *J. Mater. Chem.* **2003**, *13* (7), 1546−1553.
(19) France, R. M.; Short, R. D.; Duval, E.; Jones, F. R.; Dawson, R. A.; MacNeil, S. *Chem. Mater.* **1998**, *10* (4), 1176−1183.
(20) Kingshott, P.; Thissen, H.; Griesser, H. J. *Biomaterials* **2002**, *23* (9), 2043−2056.
(21) Griesser, H. J.; Chatelier, R. C. *J. Appl. Polym. Sci., Appl. Polym. Symp.* **1990**, *46*, 361−384.
(22) Ameen, A. P.; Short, R. D.; Ward, R. J. *Polymer* **1994**, *35* (20), 4382−4391.
(23) O'Toole, L.; Mayhew, C. A.; Short, R. D. *J. Chem. Soc., Faraday Trans.* **1997**, *93* (10), 1961−1964.
(24) O'Toole, L.; Short, R. D. *J. Chem. Soc., Faraday Trans.* **1997**, *93* (6), 1141−1145.
(25) Blattler, T. M.; Pasche, S.; Textor, M.; Griesser, H. J. *Langmuir* **2006**, *22* (13), 5760−5769.
(26) Griesser, H. J. *Vacuum* **1989**, *39* (5), 485−488.
(27) Zhang, Z.; Menges, B.; Timmons, R. B.; Knoll, W.; Förch, R. *Langmuir* **2003**, *19* (11), 4765−4770.
(28) O'Toole, L.; Beck, A. J.; Ameen, A. P.; Jones, F. R.; Short, R. D. *J. Chem. Soc.-Faraday Trans.* **1995**, *91* (21), 3907−3912.
(29) Fally, F.; Virlet, I.; Riga, J.; Verbist, J. J. *J. Appl. Polym. Sci.* **1996**, *59* (10), 1569−1584.
(30) Butler, J. E.; Ni, L.; Nessler, R.; Joshi, K. S.; Suter, M.; Rosenberg, B.; Chang, J.; Brown, W. R.; Cantarero, L. A. *J. Immunol. Methods* **1992**, *150* (1−2), 77−90.
(31) Vermette, P.; Gengenbach, T.; Divisekera, U.; Kambouris, P. A.; Griesser, H. J.; Meagher, L. *J. Colloid Interface Sci.* **2003**, *259* (1), 13−26.
(32) Su, X.; Wu, Y.-J.; Robelek, R.; Knoll, W. *Langmuir* **2004**, *21* (1), 348−353.
(33) Tayyab, S.; Haq, S. K.; Sabeeha; Aziz, M. A.; Khan, M. M.; Muzammil, S. *Int. J. Biol. Macromol.* **1999**, *26* (2−3), 173−180.
(34) Bhattacharya, A. A.; Grune, T.; Curry, S. *J. Mol. Biol.* **2000**, *303* (5), 721−732.
(35) Stenkamp, R. E.; Trong, I. L.; Klumb, L.; Stayton, P. S.; Freitag, S. *Protein Sci.* **1997**, *6* (6), 1157−1166.